Supporting Information

McAuliffe et al. 10.1073/pnas.1206400109

SI Materials and Methods

Tumor Cell Culture. Murine cell lines (4306 and 4412), human cell lines (PA-1, OVCAR5, IGROV1, OVCAR3, SKOV3, A2780, and 2008), and primary lines from patient samples (HA and ASC) were cultured in monolayer using DMEM or RPMI (Invitrogen) supplemented with 10% FBS (vol/vol) (Gemini Bio-Products) and 1% penicillin/streptomycin (vol/vol) (Invitrogen). Patient samples were obtained from the Dana Farber Cancer Institute and Brigham and Women's Hospital. Institutional Review Board approval of the study was obtained from both participating institutions. Side population (SP) analysis and immunophenotyping of cells were performed in the Flow Cytometry Cores at Joslin Diabetes Center and Brigham and Women's Hospital. Flow cytometry data were analyzed using FlowJo software.

Total RNA Isolation and cDNA Synthesis. Total RNA was isolated from cell lines and patient samples, and genomic DNA was extracted following manufacturers' instructions (Qiagen and Promega, respectively). The quality of RNA was assessed with NanoDrop1000 (Thermo Fisher Scientific Inc.) technology, and cDNA was synthesized using the SuperScript III First-Strand Synthesis System (Invitrogen).

Quantitative Real-Time PCR Analysis. Quantitative real-time PCR was conducted in triplicate for each gene of interest using SYBR Green dye and the protocol provided by SABiosciences. Gene expression levels were measured in an ABI PRISM 7300HT Sequence Detection System (Applied Biosystems). Relative quantification of target genes was calculated using the comparative cycle threshold (C_T) method ($2^{-\Delta\Delta C_T}$) with genes normalized to GAPDH. A subset of genes was verified independently using self-designed real-time PCR primer sets. All quantifications were normalized to the mRNA expression of GAPDH.

Immunofluorescence Studies. Cells were stained with a primary phospho-Histone γ-H2AX (Ser139) (20E3) rabbit mAb (Cell Signaling) using a 1:200 dilution overnight followed by a 2-h incubation with anti-rabbit IgG FAB2 Alexa Fluor (R) 488 (Cell Signaling). For quantification, 10 fields of cells were viewed at 20× magnification and positively stained γ-H2AX nuclei were counted as a percentage of total nuclei (assessed by DAPI staining).

Cell-Cycle Analysis. Treated cells were fixed overnight in 100% ethanol and then stained with propidium iodide (PI)/RNase solution (Cell Signaling) for at least 1 h before analysis by flow cytometry for PI incorporation. A total of 10,000 events were collected for final analysis. ModFit LT software (Verity Software House) was used for cell-cycle analysis.

Assessing the Efficacy of Cisplatin/γ-Secretase Inhibitor in Vivo. Drug-efficacy studies were conducted in genetically engineered K-ras$^{LSL/+}$/Pten$^{fl/fl}$/luciferase (luc) (K-ras/Pten) mouse models of ovarian cancer and SCID tumor xenografts. To generate all xenograft models, mice were injected i.p. with 2.5 million PA-1/luc, OVCAR5/luc, and SKOV3/luc cells, respectively. Animals began treatment once tumors were established, and a baseline pretreatment image was recorded for each animal. SKOV3 and PA-1 cohorts were each divided into three groups: control, cisplatin (CDDP) monotherapy, and CDDP/γ-secretase inhibitor (GSI) cotherapy. K-ras/Pten and OVCAR5 mice were each divided into four groups: control, CDDP monotherapy, GSI monotherapy, and CDDP/GSI cotherapy. Mice in each group were injected i.p. with PBS (control), CDDP (3 mg/kg of body weight), GSI (5 mg/kg of body weight), or a combination of CDDP (3 mg/kg body weight) and GSI (5 mg/kg of body weight). Treatments were administered every third day for two cycles of three treatments per cycle, for a total of six treatments. Treatment efficacy was quantified by measuring fold change in bioluminescence imaging. All studies were conducted in accordance with the Institutional Animal Care and Use Committee guidelines of the Brigham and Women's Hospital and Harvard Medical School.

Notch Overexpression and Knockdown Studies. NICDs were overexpressed in ovarian cancer cell lines to analyze the role of Notch signaling in CSC maintenance and platinum chemoresistance. All MigR1 vectors were derived from human or mouse cDNAs as previously described (1). The plasmids were transfected using a Lipofectamine protocol (Invitrogen). GFP$^+$ cells were sorted by flow cytometry 48–72 h posttransfection and were regrown in DMEM. Notch3 knockdown was accomplished using siRNA reagents and protocols from either Sigma or Santa Cruz Biotechnology, with similar results.

Statistical Analysis. The efficacy of each treatment compared with control (e.g., GSI treatment versus control), was evaluated using univariate two-tailed *t* tests and one-way ANOVA as shown before (2). GSI and CDDP monotherapies were compared with vehicle as a control; then each drug alone was compared with combination treatment. In addition, a two-way factorial ANOVA test was used to test for an interaction between GSI and CDDP. If an interaction was found ($P \leq 0.05$), and the growth inhibition was greater than seen with either treatment alone, the interaction was deemed synergistic (2). If an interaction was found ($P \leq 0.05$), and the inhibition was less than seen with either treatment alone, the interaction was deemed antagonistic or competitive (2). If no interaction was found ($P \geq 0.05$), but the effect was greater than seen with either treatment alone, the effect of the combined treatment was considered additive (2). Results determined by this method were validated further in a subset of patient samples and established cell lines (OVCAR5 and SKOV3) by an isobologram and CI analysis using CalcuSyn dose effect analysis software (Biosoft). This software package uses dose-dependent MTT assay data to calculate drug-interaction effects as described previously (3). Synergism is indicated by CI values less than 1; a CI value equal to 1 indicates an additive interaction (3). CI values higher than 1 are consistent with a competitive cytotoxic response. The CI values are shown for ED_{25}, ED_{50}, ED_{75}, and ED_{90}, as described previously (3). The CI values are provided for a wide range of CDDP and GSI effective doses.

1. Aster JC, et al. (2011) Notch ankyrin repeat domain variation influences leukemogenesis and Myc transactivation. *PLoS ONE* 6:e25645.
2. Pieretti-Vanmarcke R, et al. (2006) Mullerian Inhibiting Substance enhances subclinical doses of chemotherapeutic agents to inhibit human and mouse ovarian cancer. *Proc Natl Acad Sci USA* 103:17426–17431.
3. Taylor-Harding B, Orsulic S, Karlan BY, Li AJ (2010) Fluvastatin and cisplatin demonstrate synergistic cytotoxicity in epithelial ovarian cancer cells. *Gynecol Oncol* 119:549–556.

A

Cells Injected	10K	5K	1K	500
4306 SP	3/3	2/2	3/6	1/3
4306 NSP	1/3	1/2	0/6	0/3
4306 SP/CD44+	5/6			
4306 SP/CD44-	3/8			
4306 SP/CD44+/CD24+	2/3			
4306 SP/CD44+/CD24-	3/3			
4306 SP/CD44-/CD24+	0/2			
4306 SP/CD44-/CD24-	3/6			
OVCAR5 SP/CD44+	2/3			
OVCAR5 SP/CD44-	0/3			

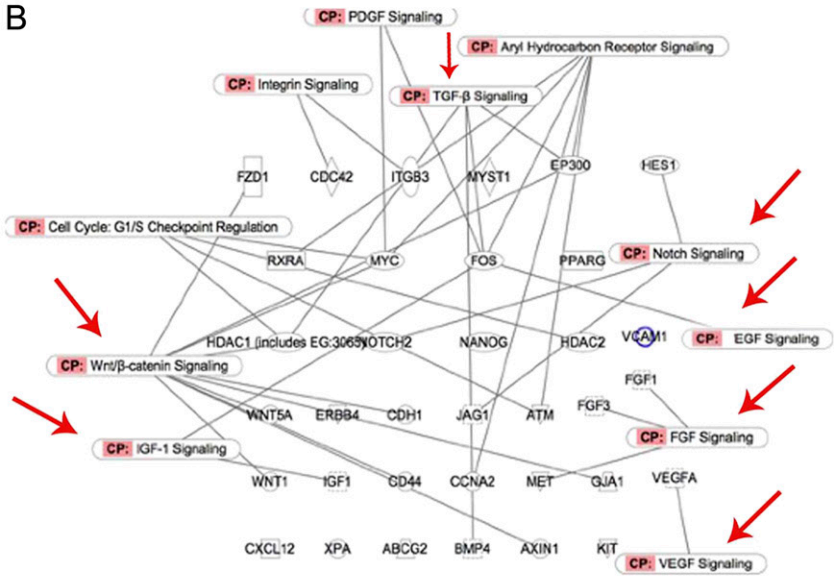

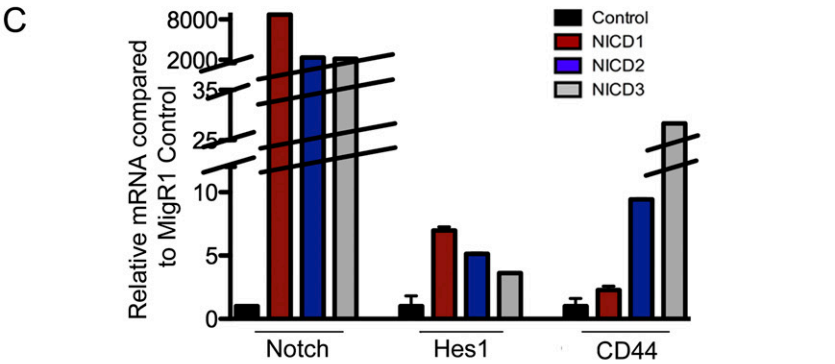

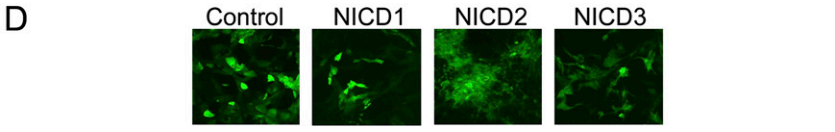

Fig. S1. Cancer stem cells (CSCs) display increased tumorigenic potential in vivo and feature key pathways that can be successfully targeted therapeutically. (*A*) SP and non-SP (NSP) cells were sorted from murine K-ras/Pten (4306) and human OVCAR5 ovarian cancer lines and injected into the right and left flanks, respectively, of SCID mice. SP cells gave rise to more tumors than did NSP cells. Injection of as few as 1,000 SP cells generated tumors in three of six mice, but injection with NSP cells did not generate tumors in any of the six mice. In addition, injection of 10,000 SP/CD44$^+$ 4306 cells generated tumors in five of six mice, but injection of SP/CD44$^-$ cells generated tumors in only three of eight mice. Similarly, injection of OVCAR5 SP/CD44$^+$ cells generated tumors in two of three mice, but injection of SP/CD44$^-$ cells did not generate tumors in any of the three mice. (*B*) Key pathways (red arrows) for ovarian CSC function were identified using Ingenuity and GeneGo's MetaCore Pathway Analysis Systems. These key signaling networks include Notch, Wnt/β-catenin, IGF1, VEGF, FGF, EGF, and TGF-β pathways. (*C*) Notch receptor intracellular domains (NICDs) were overexpressed in ovarian cancer cell lines to analyze the role of Notch signaling in CSC maintenance and platinum chemoresistance. Quantitative real-time PCR analysis demonstrates overexpression of Notch receptors (intracellular domains, NICD1–3) in transfected 4306 murine ovarian cancer cells. As expected, overexpression of NICD1–3 increases levels for Notch receptors and HES1, a Notch pathway downstream effector, as compared with MigR1 control. Furthermore, NICD3 overexpression, which increases the percent of SP cells enriched for CSCs, is also correlated with high levels of CD44 gene expression, a key stem-cell marker. (*D*) GFP expression is shown in tumor cells overexpressing NICD1–3 as a positive control for transfection levels. NICD1–3 vectors express GFP as a marker of transduced cells. GFP$^+$ cells were sorted by flow cytometry 48–72 h posttransfection and were regrown in DMEM.

A

Patient Characteristics	*N* = 99
Clinical Status	**N (%)**
Newly Diagnosed	55 (55.6)
Recurrent Disease	44 (44.4)
Tumor Subtype (Histopathology)	
Serous	82 (82.8)
Other	17 (17.2)
Sensitivity to Platinum Therapy	
Sensitive	38 (38.4)
Resistant	49 (49.5)
Incomplete follow-up data	12 (12.1)

B

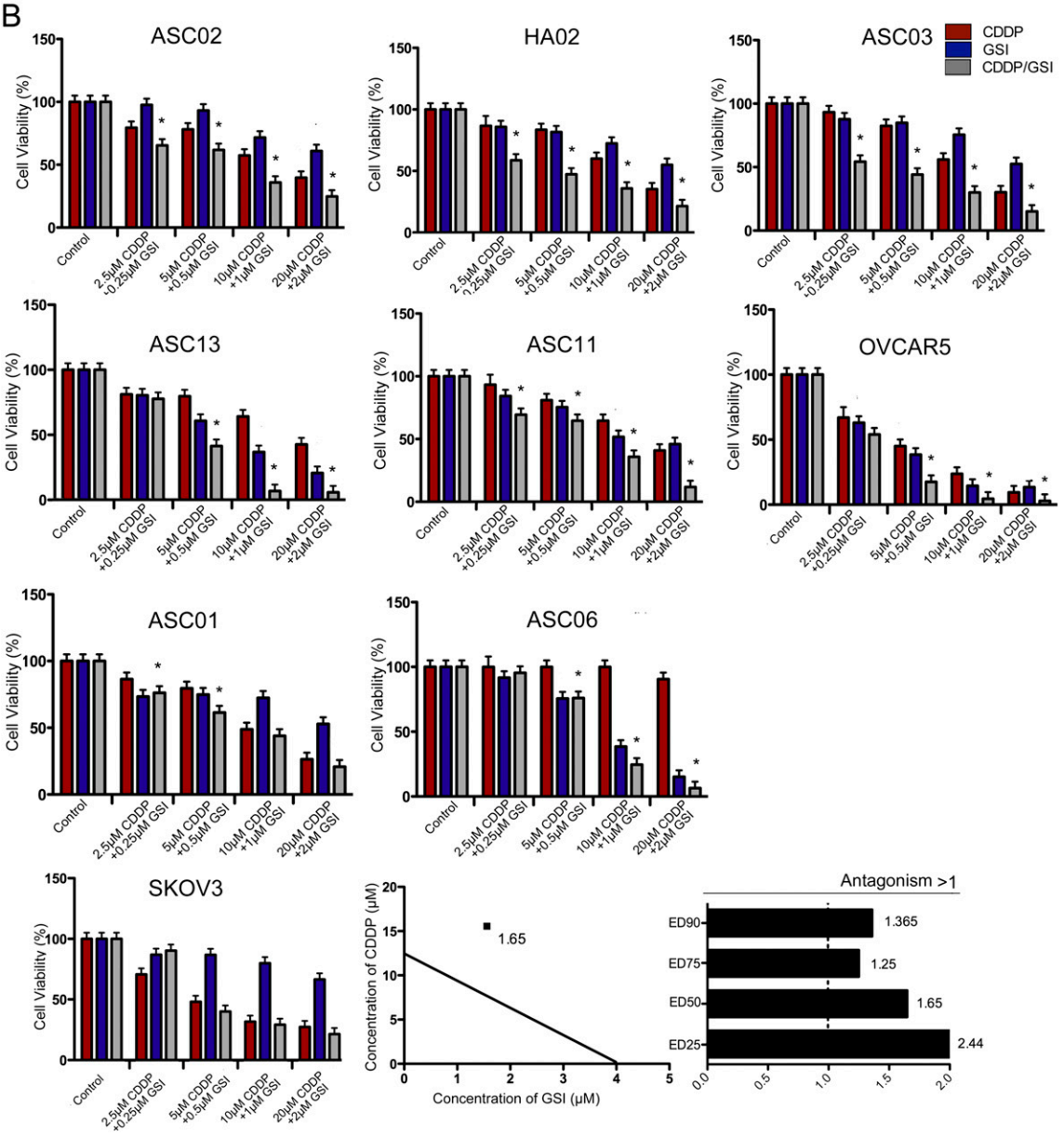

Fig. S2. Summary of patient characteristics and isobologram analysis of patient cell lines demonstrating a synergistic cytotoxic effect in vitro. (*A*) Clinical characteristics, tumor subtype (histopathology), and platinum sensitivity are shown for the patients included in the study. (*B*) Primary patient cell lines, which were analyzed previously by two-way ANOVA, were assessed further using MTT, isobologram, and combination index (CI) analysis to validate a synergistic response to GSI/CDDP therapy. Cell viability was measured by MTT assay and assessed with CalcuSyn software to provide evidence for a CDDP/GSI synergistic (ASC02, HA02, ASC03, ASC13, ASC11) or additive (ASC01, ASC06) cytotoxic response. Significant reductions in cell viability for the combination therapy in comparison with CDDP monotherapy are denoted by an asterisk (*$P < 0.05$, Student's *t*- test). Reductions in cell viability in response to CDDP or GSI monotherapy are shown in red and blue, respectively, and the combination therapy is depicted in gray. Additional established cell lines (SKOV3) were assessed using the same method. In contrast to OVCAR5, which shows a synergistic response to CDDP/GSI, SKOV3 tumor cells, in which Notch3 expression is not detected, demonstrates an antagonistic response to combination therapy (CI >1).

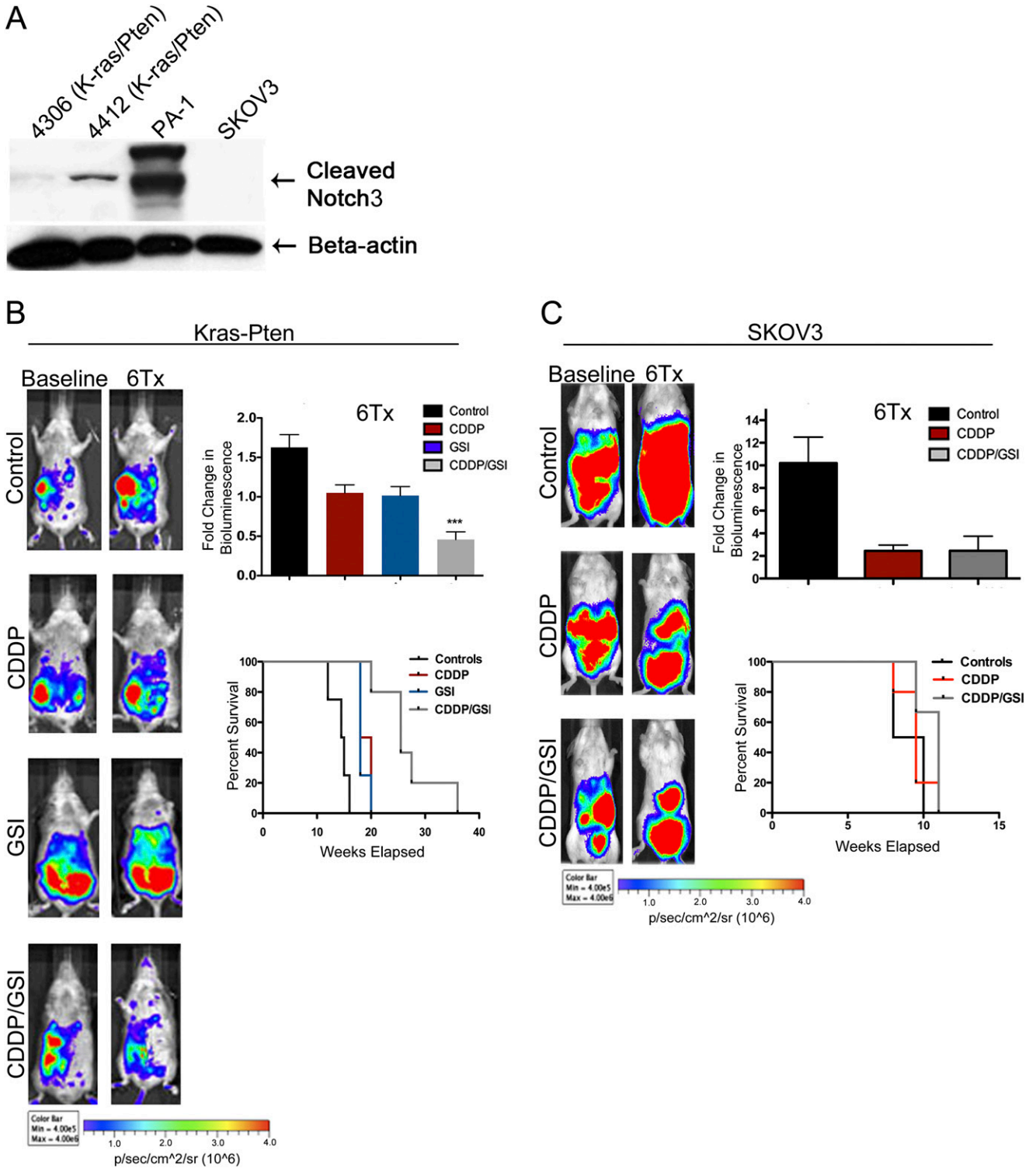

Fig. S3. GSI and platinum cotherapy significantly increases therapeutic response and survival time in K-ras/Pten/luc genetically engineered mouse models. (*A*) Western blotting analysis of Notch3 expression in murine and human ovarian cancer cell lines detects Notch3 in murine K-ras/Pten lines (4412) and human PA-1; Notch3 expression is absent in SKOV3 ovarian cancer cells. β-Actin was used as a loading control. (*B*) K-ras/Pten tumor models treated with CDDP/GSI cotherapy ($n = 8$) showed significant inhibition of disease progression (***$P < 0.001$, two-way ANOVA) and longer survival as compared with either GSI ($n = 5$) or CDDP monotherapy ($n = 4$. (*C*) In contrast, in SKOV3 tumor xenografts, in which Notch 3 is not detected, CDDP/GSI treatment ($n = 3$) shows no additional therapeutic efficacy compared with CDDP monotherapy ($n = 5$). Quantification of tumor imaging shows no significant difference between CDDP and CDDP/GSI cotherapy. Kaplan–Meier survival curves for each treatment group show that the combination therapy does not increase survival time significantly compared with CDDP monotherapy in SKOV3 tumor xenografts. 6tx, mice administered six drug treatments.

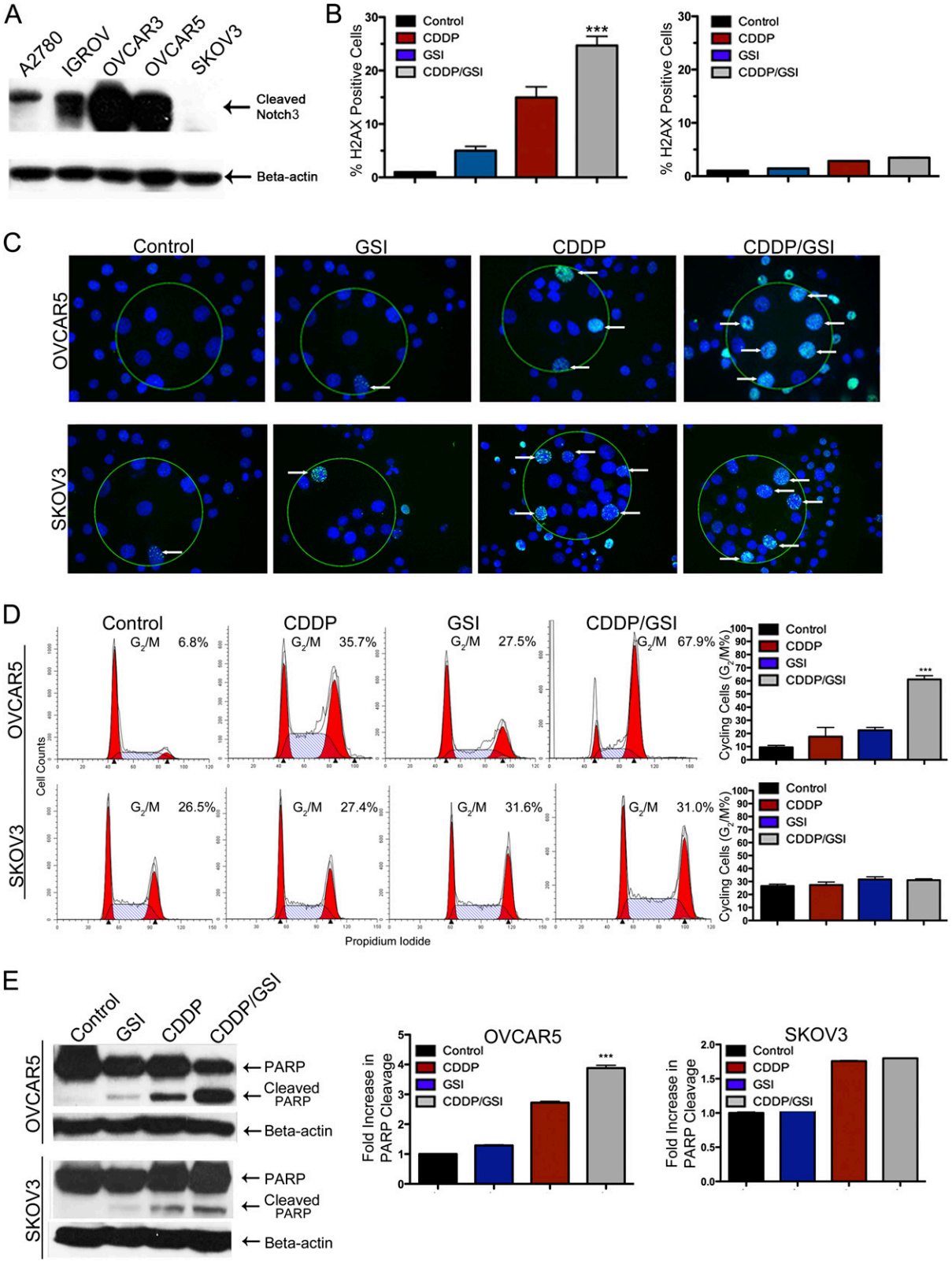

Fig. S4. GSI and platinum cotherapy shows enhanced response to DNA damage and cell death in Notch-dependent tumor cells. (*A*) Western blotting analysis of Notch3 expression in human ovarian cancer cell lines detects Notch3 overexpression in all lines (A2780, IGROV1, OVCAR3, and OVCAR5) except for SKOV3. (*B* and *C*) The response to DNA damage in human OVCAR5 and SKOV3 cells was analyzed by examining the number of γ-H2AX foci in immunofluorescence (IF) experiments. (*B*) Quantification of IF data shows that DNA damage induced by CDDP/GSI combination therapy is significantly greater (***$P < 0.001$ two-way ANOVA analysis) than seen with either monotherapy in human OVCAR5 cells expressing Notch3. In SKOV3 cells, in which Notch3 is not detected, the DNA-damage response (as indicated by the number of γ-H2AX foci) is not significantly different between the control and GSI groups or between the CDDP and

Legend continued on following page

CDDP/GSI cotherapy groups. (*C*) Representative IF slides of γ-H2AX staining for both cell lines. (*D*) The effect of the CDDP/GSI combination therapy on cell-cycle progression was determined using propidium Iodide staining and FACS analysis of human OVCAR5 and SKOV3 cells, respectively. Quantification of G_2/M subpopulations is shown as an average of four independent experiments alongside representative histograms for each cell line and treatment. GSI potentiated the G_2/M cell-cycle arrest induced by CDDP in OVCAR5 cells (***$P < 0.001$, two-way ANOVA compared with either monotherapy). In contrast, SKOV3 cells show no statistically significant increase in the G_2/M cell-cycle arrest in response to CDDP/GSI. (*E*) Accumulation of poly(ADP-ribose) polymerase (PARP) cleavage, a marker of cell death, was quantified by Western blotting analysis in OVCAR5 and SKOV3 cells that were treated with GSI, CDDP, or CDDP/GSI combination therapy. OVCAR5 cells treated with CDDP/GSI combination therapy show a significant increase in PARP cleavage compared cells treated with either monotherapy (***$P < 0.001$, two-way ANOVA), whereas in SKOV3 cells PARP cleavage in response to CDDP/GSI is not significantly increased compared with CDDP alone. β-Actin is shown as a loading control for tumor lysates.